Saudi Pharmaceutical Journal 27 (2019) 491–501

Contents lists available at ScienceDirect

Saudi Pharmaceutical Journal

journal homepage: www.sciencedirect.com

Original article

Nano-encapsulation and characterization of baricitinib using poly-lactic-glycolic acid co-polymer

Mohammad Javed Ansari *, Saad M. Alshahrani

Department of Pharmaceutics, College of Pharmacy, Prince Sattam Bin Abdulaziz University, Alkharj, Saudi Arabia

ARTICLE INFO

Article history:
Received 15 November 2018
Accepted 10 January 2019
Available online 12 January 2019

Keywords:
Baricitinib
Nanoparticles
Nanoprecipitation
Encapsulation
Solubility
Dissolution

ABSTRACT

Baricitinib is a recently approved anti-rheumatic drug having very poor aqueous solubility and hence its performance suffers from low or inconsistent oral bioavailability. The purpose of the study was to develop and evaluate poly lactic-co-glycolic acid (PLGA) nanoparticles of baricitinib in order to enhance *in vitro* dissolution and performance. Nano-suspension of baricitinib with or without PLGA, a biodegradable, FDA approved semi-synthetic polymer, was developed by nanoprecipitation method. Research methodology employed a quantitative research utilizing experimental design wherein effect of independent variables such as amount of polymer, drug: polymer ratio, types of solvent, and solvent: anti-solvent ratio were evaluated over the size and size distribution of nanoparticles along with entrapment efficiencies. Among the several organic phases evaluated, acetone was found to be suitable solvent for drug and polymer. The aqueous phase (anti-solvent) was deionized water containing 1% w/v pluronic 127 as the stabilizer of nanoparticle suspension. The optimized nanoparticles had particle size less than 100 nm (91 nm ± 6.23) with a very narrow size distribution (0.169 ± 0.003), high zeta potential (−12.5 mV ± 5.46) and entrapment efficiency (88.0%). The optimized nanoparticles were characterized by scanning electron microscopy, X-ray diffraction, differential scanning calorimetry, infrared spectroscopy and *in vitro* dissolution studies. *In-vitro* dissolution study of PLGA nanoparticles exhibited sustained release with approximately 93% release of baricitinib during 24-h period.

1. Introduction

Rheumatoid arthritis is an autoimmune disorder that causes inflammation of joints such as knees, ankles, hands and feet which leads to swelling, pain and immobility (Aletaha et al., 2010). Treatment options available to treat this disease include nonsteroidal anti-inflammatory drugs (NSAID), corticosteroids, disease-modifying anti-rheumatic drugs (DMARD) and injectable biologics. Baricitinib, a new sub-class of DMARD, has recently been approved as oral immediate release tablets by USFDA for the treatment of rheumatoid arthritis especially for the patients not responding to the available therapies (Drug Approval Package: Olumiant baricitinib, 2018). It is a selective inhibitor of Janus kinase 1 and 2 (JAK 1 and JAK 2). Janus kinases are group of enzymes that activate signal transducers and activators of transcription enabling the inflammation and immune function (Assessment report Olumiant, 2018). Baricitinib is an aromatic polyheterocyclic compound (Fig. 1a) with molecular formula and molecular weight as $C_{16}H_{17}N_7O_2S$ and 371.42 respectively (Assessment report Olumiant, 2018). As per assessment report, baricitinib belongs to class III of biopharmaceutical classification system (BCS), which means that it is highly soluble and poorly permeable drug, however, the same report also mentioned that baricitinib is practically insoluble. (Assessment report Olumiant, 2018). Nevertheless, it has been reported to have both solubility (0.357 mg/ml of water) as well as permeability (Log P = 1.08) challenges as per drugbank identification report (Drugbank: identification of baricitinib, 2018). Baricitinib has been reported to be soluble in organic solvents such as dimethyl sulphoxide (74 mg/ml), dimethyl formamide (50 mg/ml) but very poorly soluble in water and ethanol (<1 mg/ml at 25 °C) (Baricitinib: technical information, 2018). Another product information on baricitinib reported poor aqueous solubility of baricitinib (~0.5 mg/ml in 1:1 mixture of phosphate buffer saline pH 7.2: dimethyl formamide) while solubility in organic solvents like such as dimethyl sulphoxide and dimethyl formamide was

* Corresponding author.
E-mail addresses: mj.ansari@psau.edu.sa (M.J. Ansari), sm.shahrani@psau.edu.sa (S.M. Alshahrani).
Peer review under responsibility of King Saud University.

Production and hosting by Elsevier

https://doi.org/10.1016/j.jsps.2019.01.012
1319-0164/

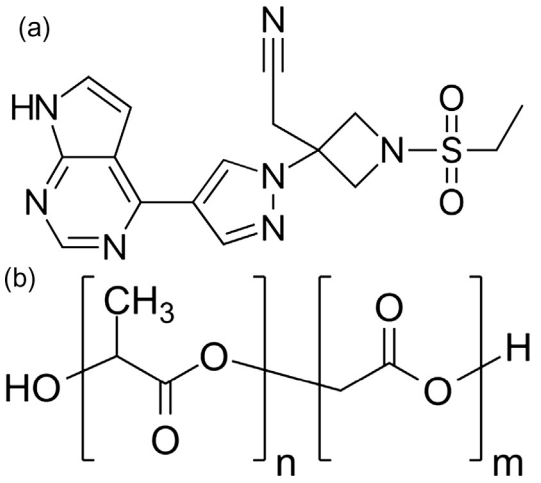

Fig. 1. Molecular structures of (a) baricitinib and (b) Poly (lactic-co-glycolic acid), n = number of units of lactic acid; m = number of units of glycolic acid.

~50 mg/ml (Product information: baricitinib, 2018). Drugs with poor solubility or permeability suffer with low and or inconsistent bioavailability affecting the performance and therapeutic goals (Dahan and Miller, 2012). Moreover, low bioavailability necessitates administration of higher doses that may lead to side effects. Oral bioavailability of aqueous solution of baricitinib in 0.5% methylcellulose was reported as 48% in dogs, 54% in rats, 47–68% in monkey and 79% in human (Assessment report Olumiant, 2018). Pharmacokinetic parameters such as Cmax, Tmax, AUC0-∞, total clearance and elimination half-life after oral administration of baricitinib in healthy volunteer were reported as ~112 nM, ~1h, 740 nM × h, ~17 L/h and ~8 h respectively (Assessment report Olumiant, 2018). The inter-subject variability of pharmacokinetic parameters was reported to be moderate with a range between 17 and 26% in healthy volunteers while in patients with rheumatoid arthritis it was as high as 41% (Assessment report Olumiant, 2018).

There are various techniques to improve solubility and bioavailability of such drugs. Polymeric nanoparticles based on PLGA (Fig. 1b) have been investigated extensively for the enhancement of solubility or bioavailability of poorly soluble drugs due to certain advantages such as biodegradable and biocompatible nature of the copolymer. Moreover, it is non-immunogenic, nontoxic, and approved by FDA for various biomedical and pharmaceutical applications (Makadia and Siegel, 2011). The recent literature search revealed that PLGA is one of the most widely used polymeric materials employed for the fabrication of nanoparticles. It has been reported to enhance solubility and bioavailability of several poorly soluble drugs such as resveratrol (Singh and Pai, 2014), nelfinavir (Venkatesh et al., 2015), lopinavir (Joshi et al., 2016), docetaxel (Rafiei, and Haddadi, 2017) and benzophenone (Costabile et al., 2018).

This study has been undertaken to develop and evaluate baricitinib encapsulated PLGA nanoparticles to improve dissolution and performance of the drug. There is no report on the investigation of solubility or bioavailability of baricitinib encapsulated PLGA nanoparticles.

2. Materials and methods

2.1. Materials

Baricitinib was purchased from Mesochem Technology Co Ltd (Beijing, China). PLGA polymer (50:50), Pluronic acid 127 and was purchased from Sigma–Aldrich (St. Louis, MO). Acetone (AC), acetonitrile (AN), dichloromethane (DCM), ethylacetate (EA) and tetrahydrofuran (THF) were of analytical grade and were purchased from Sigma–Aldrich (St. Louis, MO). Deionized water was obtained from Milli-Q, Millipore, Massachusetts USA.

2.2. Methods

The research methodology employed a quantitative research utilizing experimental design wherein effect of the dependent variables such as nanoparticle size, size distribution (polydispersity index-PDI), zeta potential and entrapment efficiency over the independent variables such as amount of polymer, drug, type of solvent, and solvent: anti-solvent ratio were investigated.

2.3. Formulation of baricitinib encapsulated nanoparticles

Baricitinib encapsulated PLGA nanoparticles were prepared by nanoprecipitation method which involves precipitation of insoluble drugs in the aqueous phase when an organic solution of drug and polymer mixture is added slowly to the aqueous phase kept on moderate stirring (Fessi et al., 1989). Definite amount of baricitinib and PLGA were dissolved in suitable organic solvent which was then added dropwise in anti-solvent kept over moderate stirring of 700 rpm. The mixture was stirred over night to remove the organic solvent that rendered hardening of nanoparticles. Nanosuspension was centrifuged at 15000 × rcf (Centurion scientific, UK) for 30 min to separate the nanoparticles, which was then washed with cold water and freeze- dried (Mill rock technology, Kingston, NY) for further analyses.

2.3.1. Effect of solvent

Various organic solvents like acetone (AC), acetonitrile (AN), dichloromethane (DCM), ethyl acetate (EA) and tetrahydrofuran (THF), were investigated to optimize the organic phase for nanoprecipitation. Accurately weighed PLGA (50 mg) and baricitinib (10 mg) was dissolved separately in 10 ml of each organic solvent to prepare different formulation with formulation codes (F1–F5) as presented in Table 1. The prepared organic phases were added dropwise to the 50 ml of anti-solvent (1% aqueous pluronic 127) kept over magnetic stirrer rotating at 700 RPM.

2.3.2. Effect of anti-solvent

To investigate the effect of anti-solvent on nanoprecipitation, different ratio of solvent: anti-solvent (1:2, 1:3, 1:5 and 1:10) were investigated for optimization of the nanoparticles. Accurately weighed baricitinib (10 mg) and PLGA (50 mg) were dissolved in 10 ml of acetone as a solvent for both drug and polymer. The deionized water was used as anti-solvent containing 1% pluronic 127 as stabilizer. The composition of the formulations (F6-F9) are presented in Table 2.

2.3.3. Effect of polymer

To investigate the effect of polymer on the formulation characteristics, the polymer concentration was varied in the range

Table 1
Formulation codes and composition of nanoparticles containing 10 mg of baricitinib and 50 mg of PLGA.

Formulation number	Organic solvent	Formulation code
F1	Acetone	AC
F2	Acetonitrile	AN
F3	Dichloromethane	DCM
F4	Ethyl acetate	EA
F5	Tetra hydro furan	THF

Table 2
Formulation codes and composition of nanoparticles containing 10 mg of baricitinib and 50 mg of PLGA prepared with varying solvent and anti-solvent ratio.

Formulation number	Formulation code	Solvent (ml)	Anti-solvent (ml)
F6	S:AS/1:2	10	20
F7	S:AS/1:3	10	30
F8	S:AS/1:5	10	50
F9	S:AS/1:10	10	100

between 1 and 10 mg/ml of acetone. The organic phase containing 10 mg of baricitinib and different amount of PLGA in the range of 1–10 mg/ml were prepared in 10 ml of acetone to have different formulations (F10–F13) as presented in Table 3. The prepared organic phases were then added dropwise to the 50 ml of anti-solvent (1% aqueous pluronic 127) kept over magnetic stirrer rotating at 700 RPM.

2.3.4. Effect of drug

The effect of drug on the particle size, size distribution and zeta potential were investigated by preparing formulations with or without drug and or polymer. The composition of the formulations (F14–F16) are presented in Table 4. The component (s) were dissolved in 10 ml of acetone to prepare organic phases (except F-16, which was prepared by suspending 10 mg of baricitinib in 1% pluronic 127 for comparison purpose). The prepared organic phases were added dropwise to the 50 ml of anti-solvent (1% aqueous pluronic 127) kept over magnetic stirrer set at 700 RPM.

2.4. Optimization of nanoparticles

The prepared nanoparticle formulations were optimized on the basis of visual appearance (agglomeration), particle size, size distribution (polydispersity index), zeta potential and % entrapment efficiency.

2.4.1. Particle size and size distribution

The particle size and size distribution was investigated by dynamic light scattering (DLS) technique, wherein fluctualtions in the intensity of scattered light is measured as a function of movement (diffusion) of nanoparticles. The smaller the nanoparticles, the faster will be the diffusion (Brownian motion), as described by Eq. (1), derived from Stoke-Einstein diffusion equation (Eq. (2)). Faster diffusion of the nanoparticles result in rapid fluctualtions in the scattered light. These fluctuations in the scattered light is then measured by a photon counter and correlated with the diffusion coefficient of nanoparticle (hydrodynamic size of nanoparticle) therefore DLS technique is also called as photon correlation spectroscopy (PCS). In this study, we employed state of the art equipment, Zetasizer Nano ZS, model ZEN3500 (Malvern Instruments, UK), for particle size and size distribution measurement. It utilizes a patented non-invasive back scatter (NIBS) technology that measures the scattered light at a backscatter angle of 173° improving it's sensitivity and measuring capacity. The nanoparticles (~5 mg) were suspended in 10 ml of deionized water by vortex mixing for 30 s followed by ultrasonication for 60 s to break agglomerates if any. Appropriate volume, approximately 2 ml of the prepared nanoparticle suspension was taken in the disposable plastic cuvette. Particle size was then measured in triplicate at 25 °C. The size of nanopartilces is reported as Z-average diameter (Eq. (3)), an intensity based harmonic mean diameter calculated by cumulant analysis using least squares fitting, therefore considered as relatively insensitive to experimental noise (Finsy and De Jaeger, 1991).

$$R = \frac{k_B T}{6\pi\eta D} \tag{1}$$

where,

R = Hydrodynamic radius of the nanoparticle,
k_B = Boltzman's constant,
T = Temperature,
η = Viscosity of the dispersion medium,
D = Diffusion coefficient

$$D = \frac{k_B T}{6\pi\eta R} \tag{2}$$

$$Dz = \frac{\sum Si}{\sum (Si/Di)} \tag{3}$$

where

Dz = Z average diameter,
Si = Scattered intensity from nanoparticle i
Di = Diameter of nanoparticle i.

2.4.2. Evaluation of zeta potential of nanoparticle suspension

The zeta potential of disperse systems such as nanoemulsions and nanosuspensions is one of the very important characteristics that helps in stability of the dispersions. It is potential difference across the phase boundaries between dispersed phase and dispersion medium. It is considered as an index of repulsion, thus higher the zeta potential, higher will be repulsion between the dispersed particles with similar charges resulting in more stable dispersions. The magnitude of zeta potential mainly depends on the charges over the dispersed phase and in the dispersion medium, which in turn is influenced by dielectric constant/ionic strength, conductivity, viscosity and pH of the dispersion medium as described by Henry equation (Eq. (4)). Therefore, evaluation of the zeta potential of nanoparticle suspension becomes very important to predict its fate such as stability, transportation or absorption within the body/body tissues. Zeta potential of nanoparticles is determined experimentally by measuring the electrophoretic mobility of the nanoparticles i.e. measurement of velocity of nanoparticles moving towards electrodes under electrical fields. The higher the velocity, the higher will be the magnitude of zeta potential. In this study, we used zetasizer nano ZS (Malvern Instrument, UK) with patented mixed mode measurement, phase analysis light scattering (M3-PALS), which is capable of measuring mean zeta potential and zeta potential distribution with excellent accuracy. Briefly, the nanoparticles (~5 mg) were suspended in 10 ml of 10 mM sodium chloride by vortex mixing (30 s) followed by ultrasonication for

Table 3
Formulation codes and composition of nanoparticles containing 10 mg of baricitinib and varying amounts of PLGA dissolved in 10 ml of acetone.

Formulation number	Formulation code	polymer concentration (mg/ml)	polymer amount (mg)
F10	PLGA 1	1	10
F11	PLGA 2	2	20
F12	PLGA 3	3	30
F13	PLGA 10	10	100

Table 4
Formulation codes and composition of nanoparticles with or without baricitinib and or PLGA dissolved in 10 ml of acetone.

Formulation number	Formulation code	Baricitinib (mg)	PLGA (mg)
F14	D:P/1:0	10	0
F15	D:P/0: 1	0	10
*F16	D: P/1:0	10	0

* F-16 was prepared by suspending the drug in 1% pluronic 127.

60 s to break agglomerates if any. The appropriate volume (~0.9 ml of nanosuspension) was then introduced with the help of syringe into specialized polycarbonate zeta cells (folded capillary cell with gold-plated electrodes, model DTS1017, Malvern Instruments) held in inverted position to avoid introduction of air bubbles. Caps for zeta cells were used to close the cell. Zeta potential was then measured in triplicate at 25 °C.

$$\mu e = \frac{2z\varepsilon f(ka)}{3\eta} \quad (4)$$

μe = electrophoretic mobility,
z = zeta potential,
ε = dielectric constant,
f(k a) = Henrys function; it equals to 1.5 (for polar dispersant); known as the Smoluchowski approximation.
η = viscosity of the dispersion medium.

2.4.3. Drug entrapment efficiency of nanoparticles

The drug entrapment efficiency of the nanoparticle formulations was calculated by indirect method which involded sedimentation of nanoparticles by ultracentrifugation followed by analysis of unentrapped drug in the supernetant. The difference between the amount of drug added initially in the formulation and unentrapped drug found in the supernetant gives the amount of drug entrapped in formulation. Briefly, nanoparticle suspensions were centrifuged at 15000 × rcf for 30 min. The supernetant obtained was analyzed by bouble beam UV spectrophotometer (UV 630, Jasco, Japan) at 224 nm after appropriate dilution. The % entrapment efficiency of the formulation was calculated as mentioned in Eq. (5).

$$\%Entrapment = \frac{Drug\ loaded\ -\ Drug\ found}{Drug\ loaded} X100 \quad (5)$$

The drug loading capacity were calculated by direct method which involved comparison of practically loaded drug found in analysis of nanoparticle solution with that of theoretical amount of drug taken in beginning to load in the polymer (Eq. (6)). Briefly, about 10 mg of dried nanoparticles were dissolved in acetone which was then diluted appropriately and analyzed by double beam UV spectrophotometer (UV 630, Jasco, Japan) at 224 nm.

$$\%Drug\ loading = \frac{Amount\ of\ drug\ found}{Amount\ of\ drug\ and\ polymer} X100 \quad (6)$$

2.5. Characterization of baricitinib encapsulated PLGA nanoparticles

The characterization of optimized nanoparticle was carried out by studying the size and surface morphology by Scanning Electron Microscopy (SEM), powder properties by X-ray Diffractrometry (XRD), Differential Scanning Calorimetry (DSC), Fourier Transform Infra Red spectroscopy (FT-IR), *in vitro* drug release studies and release mechanism.

2.5.1. Size and surface characterization

The size and surface of baricitinib encapsulated nanoparticles were characterized by Scanning Electron Microscopy (Zeiss EVO LS10; Cambridge, UK). The dried nanopartilces were suspended in one ml of deionized water and sonicated for 1 min to break the agglomeration if any. A drop of nanoparticle suspension was fixed on the carbon tape (SPI Supplies, West Chester, PA) and gold coated under vacuum (Q150R sputter coater, Quorum Technologies Ltd, East Sussex, UK) in an argon atmosphere at 20 mA for 60 s (Alshehri et al., 2017).

2.5.2. X-ray diffractometry (X-RD) of nanoparticles

The X-ray diffractometry of the pure baricitinib and baricitinib encapsulated PLGA nanopartilces was conducted to compare powder characteristics before and after nanoencapsulation using Altima IV, X-ray diffractometer (Rigaku, Japan). The appropriate amount of dried nanopartilces and pure drug samples were placed on the XRD sample holder and pressed with help of glass slide. The X ray diffraction patterns at 2θ were then obtained by scanning the samples between 5° and 60° at a step size and step time of 0.02° and 0.5 s respectively (Ansari, 2016).

2.5.3. Differential scanning calorimetry (DSC)

The differential scanning calorimetry of the drug and drug encapsulated nanoparticles was carried out by using DSC-N 650 (SCINCO, Italy). Approximately 5 mg of pure drug sample and drug encapsulated nanoparticles were crimped into aluminum pans. Empty aluminum pan was crimped similarly to be used as reference material. The sample and the reference were then p laced in sample holder and scanned between 50 and 250 °C at a rate of 10 °C per minute with nitrogen gas flowing at 20 ml per minute.

2.5.4. Fourier transform infra-red spectroscopy (FT-IR)

Fourier transform infra-red spectroscopy of the drug and drug enclosed nanoparticles was conducted by using the potassium bromide (KBr) disc technique on the FT-IR instrument (FT/IR-4600, Jasco, Japan). Approximately 5 mg of drug or drug encapsulated nanoparticles was mixed and triturated with equal amount of KBr in mortar. The obtained mixtures were then compressed by Quick Press KBr pellet kit to obtain thin films. The sample film is mounted in sample holder and scanned between a wavenumber range of 400–4000 cm^{-1} after taking background scan.

2.5.5. In vitro release study

In vitro release study of nanoparticles was performed by sample and separate method (Shen and Burgess 2013). The nanoparticle sample containing ~10 mg drug was weighed and introduced into 25 ml of release media (phosphate buffer pH 6.8, containing 0.5% w/v of Sodium lauryl sulphate) kept on thermostated (37 ± 1 °C) biological shaker rotating at 100 RPM (LBS-030S-Lab Tech, Korea). An aliquot of 1 ml was sampled at 0, 0.5, 1, 2, 4, 8, 12, and 24 h after the addition of nanoparticles in release media. Fresh media was introduced after every sampling to maintain the sink condition. Withdrawn samples were centrifuged at 15,000 rcf for 30 min then analyzed by double beam UV spectrophotometrically at 224 nm. The release kinetics (mechanism of drug release) of nanoparticles were studied by fitting the release data to zero order, first order, Higuchi and Korsmeyer-Peppas plots (Mu and Feng, 2003). The release rate constants k and n of the models were calculated by linear regression analysis.

3. Results and discussions

3.1. Formulation of baricitinib encapsulated PLGA nanoparticles

Fabrication of baricitinib encapsulated PLGA nanoparticles were achieved by nanoprecipitation method (Fessi et al., 1989). It is one of the simplest methods of fabrication of nanopartilces based on bottom up technology. It involved solubilization of baricitinb and PLGA in a suitable organic solvent followed by slow addition of the prepared organic phase into aqueous phase resulting in nanoprecipitation. We prepared several formulations and investigated the effect of various independent variables such as amount of PLGA, baricitinib: PLGA ratio, nature of organic solvent, and solvent: anti-solvent ratio on the fabrication of nanoparticles.

3.2. Optimization of baricitinib encapsulated nanoparticles

The development and optimization of nanoparticles were performed by investigating the effect of several independent variables such as amount of polymer, amount of drug, types of solvent and anti-solvent with varying ratio over the dependent variable such as size, size distribution, zeta potential and entrapment efficiency of nanoparticle suspension.

3.2.1. Effect of solvent

Several solvents were investigated to select the optimum solvent for nanoprecipitation based on absence of agglomeration and parameters such as nanoparticle size, size distribution, zeta potential and entrapment efficiency. Formulation 1 (F1) containing acetone was optimized and selected as solvent for polymer and drug based on absence of agglomeration, the lowest size (120 nm), smallest PDI (0.091), the highest zeta potential (−8.5 mv) and good entrapment efficiency (Fig. 2). The entrapment efficiency of formulation in acetonitrile (F-2) and dichloromethane (F-3) were higher with 93.2% and 91.9% respectively. However, these formulations were not chosen as optimum owing to larger nanoparticle size (PDI) of 964 nm (0.804) and 608 nm (0.643) for F-2 and F-3 respectively. The effect of solvent on the size, size distribution and entrapment efficiency of nanoparticles is not well understood. Smaller sizes of nanoparticles in formulation F-1 may be ascribed to better solubility of PLGA in acetone and better diffusion of acetone in the anti-solvent compared to other solvents. Moreover, low boiling point, high dielectric constant and high water miscibility of acetone may be advantageous in producing smaller size nanoparticles (Huang and Zhang 2018).

3.2.2. Effect of anti-solvent

Various ratio of solvent: anti-solvent (1:2, 1:3, 1:5 and 1:10) were tested for optimization of the nanoparticles based on size, PDI, zeta potential and entrapment efficiency. Decrease in the solvent:antisolvent ratio from 1:2 to 1:5 resulted in reduction of particle size and PDI but at the cost of loss in the entrapment efficiency. Further decrease in the phase ratio resulted in larger nanoparticles with higher entrapment efficiency. A solvent: anti-solvent ratio of 1:5 (formulation number F-8) was chosen as the optimum formulation based on the smallest size (91 nm), the lowest PDI (0.169), the highest zeta potential value (−12.5) with entrapment efficiency of 88.0% (Fig. 3). The smaller sizes of nanoparticles at smaller solvent:antisolvent ratio could be attributed to low viscosity of the mixture and better diffusion of solvent in the antisolvent (Sahu and Das, 2014).

3.2.3. Effect of concentration of PLGA on nanoparticles

Organic solutions of PLGA with various concentration were investigated for optimization of the nanoparticles based on size, PDI, zeta potential and entrapment efficiency. Increasing concentration of polymer in organic solution resulted in increase in size and entrapment efficiency of the nanoparticles (Fig. 4). Formulation F-10 that contains the lowest concentration of PLGA (1 mg/ml of in acetone) resulted in the smallest nanoparticles (88 nm) but with the lowest entrapment efficiency (69.1%). Formulation F 14, with highest concentration of PLGA (10 mg/ml in acetone) exhibited the highest drug entrapment efficiency (90.8%) but at the cost of comparatively larger nanoparticles (158 nm). This increase in the size of nanoparticles, upon the increment of PLGA concentration in the acetone, may be due to the increased viscosity that might have reduced the diffusion of PLGA form acetone to the anti-solvent (Ansari, 2017).

3.2.4. Effect of drug and polymer on the nanoparticles

The effect of drug on the particle size, size distribution and zeta potential was investigated by preparing formulations with or without drug and or polymer (Fig. 5). The nanoparticles of drug alone (formulation F-14) prepared by nanoprecipitation of organic solution of baricitinib resulted in large nanoparticles (427 nm) with high PDI (0.46) and low zeta potential (−8.6 mV). Similarly, nanoparticles of polymer alone (formulation F-15) prepared by nanoprecipitation of organic solution of PLGA resulted in larger nanoparticles (635 nm) with higher PDI (0.86) and lower zeta potential (−5.5 mV). The larger size of nanoparticles with very high PDI and very low zeta potential are indicative of particle growth or aggregation which could be due to absence of polymer. Polymeric materials present in organic phase (formulation F1–F13) prevent aggregation of nanosuspension by forming a layer around the nanoprecipitates once it is formed thus control and stabilize the size of particles. The mechanism of stabilization of size of nanoparticles could include either steric stabilization or electrostatic

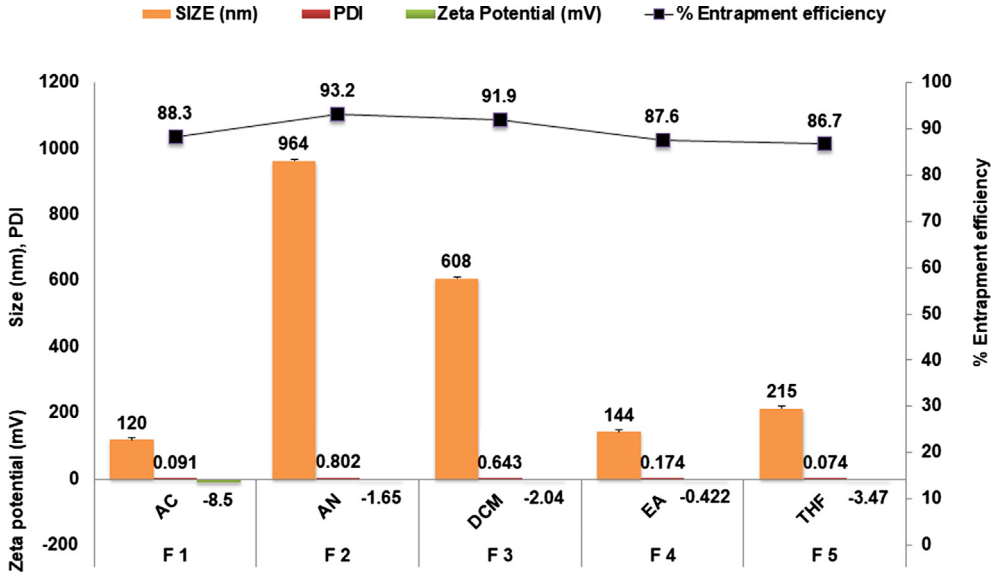

Fig. 2. Effect of solvent on the size, poly dispersity index (PDI), zeta potential and entrapment efficiency of baricitinib encapsulated PLGA nanoparticles. AC – acetone, AN – acetonitrile, DCM – dichloromethane, EA – ethyl acetate and THF – tertahydrofuron.

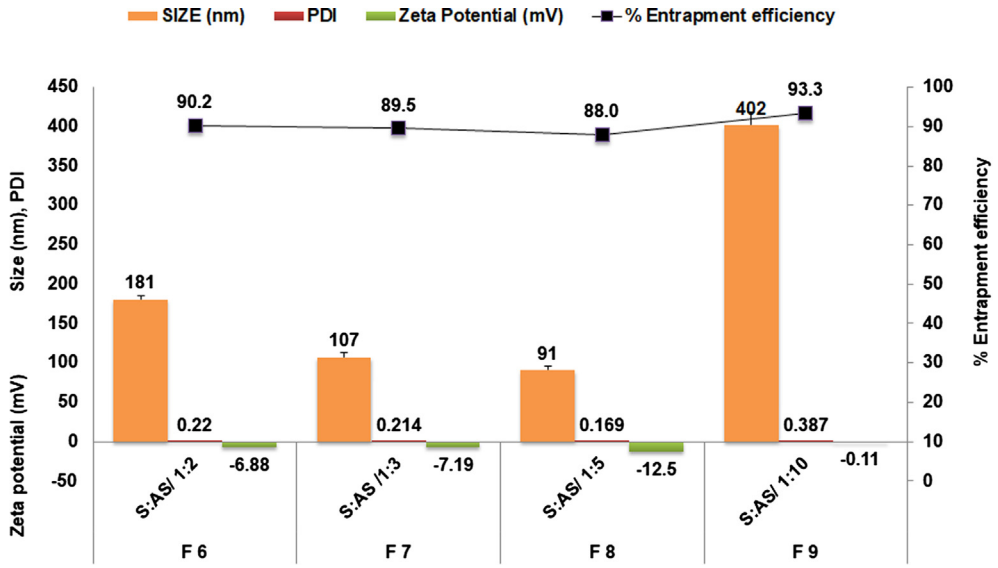

Fig. 3. Effect of solvent: anti-solvent ratio on the size, poly dispersity index (PDI), zeta potential and entrapment efficiency of baricitinib encapsulated PLGA nanoparticles.

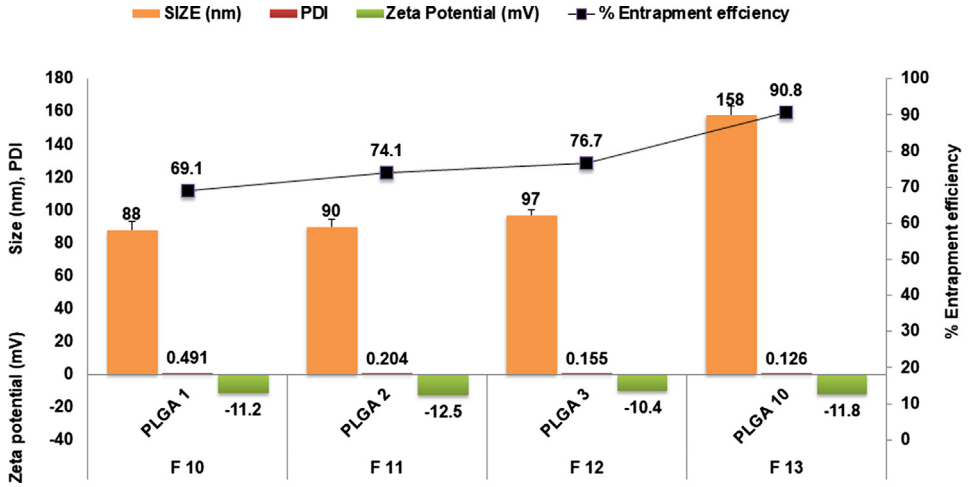

Fig. 4. Effect of PLGA concentration on the size, poly dispersity index (PDI), zeta potential and entrapment efficiency of baricitinib encapsulated PLGA nanoparticles.

repulsion due to presence of surface charges or a combination of both. The drug suspension (F16) exhibited even poorer particle characteristics with average particle size of 935 nm, the highest PDI (0.96) and the lowest zeta potential value (−1.1 mV).

Based on the combined effect of types of solvent, solvent: anti-solvent ratio (phase ratio) and PLGA concentration (drug: polymer ratio) over the desired properties of nanoparticles such as the lowest size, the lowest PDI, the highest zeta potential and high entrapment efficiency, formulation F-8 was selected as optimized formulation for further evaluations. The smaller nanoparticles are known to be absorbed or up taken by mucosal cells better than their larger counterparts (Win and Feng, 2005). The particle size, PDI and zeta potential of nanoparticles were evaluated by zeta sizer nano ZS (Malvern, UK). An image of size analysis and zeta potential analysis of F-8 is presented in Fig. 6 and Fig. 7 respectively.

The characterization of nanoparticle suspension in term of zeta potential is one of most important tool for prediction of stability of dispersions. It is considered as an index of repulsion, thus the more is the value of zeta potential, the more will be stability of nanosuspension. A higher zeta potential means higher electric charge on the surface of the NPs that prevents aggregation of the nanoparticles. In the present investigation, we found an average zeta-potential of around −10.5 mV for all the prepared formulation with the value of −12.5 ± 5.6 mV for the optimized one (F-8). It has been reported that absolute Zeta potential values above 30 mV provide good stability (Jiang et al., 2009). However, large molecular weight solids or polymers are known to stabilize the suspensions by steric hindrance despite of low zeta potential (Honary and Zahir, 2013).

3.3. Characterization of nanoparticles

The characterization of optimized nanoparticle formulation (F-8) was carried out by studying the size and surface morphology by SEM, powder properties by XRD, FT-IR, DSC and drug release study and release mechanism.

3.3.1. Size and surface characterization

The size and surface of nanoparticles were further characterized by Scanning Electron Microscopy (Zeiss EVO LS10; Cambridge, UK). The SEM photographs of baricitinib encapsulated PLGA nanoparticles (F8) are shown in Fig. 8. The size of the nanoparticles were in

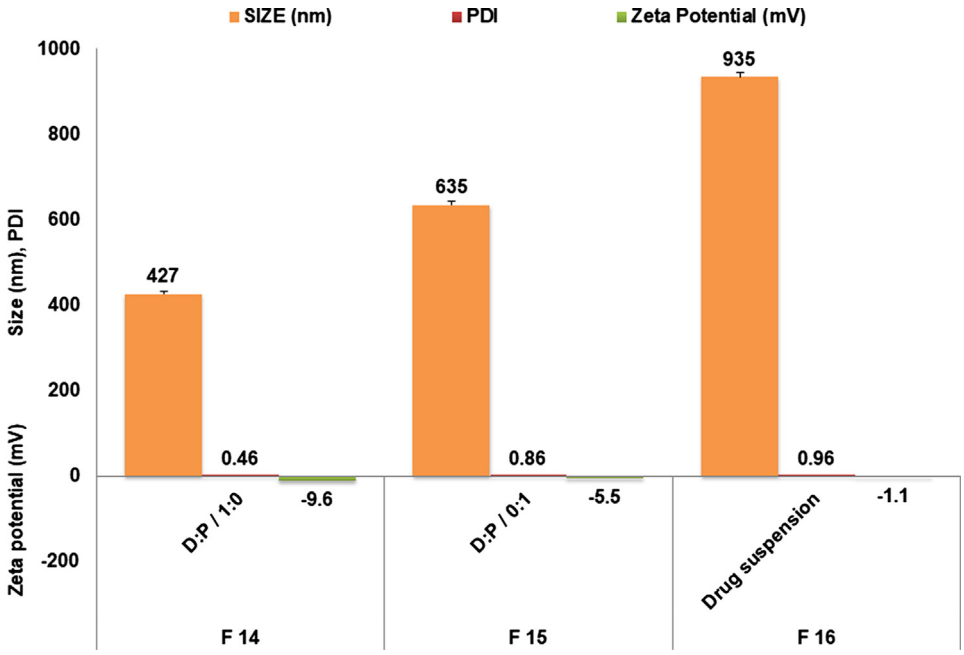

Fig. 5. Effect of the drug and or polymer on the size, poly dispersity index (PDI), zeta potential and entrapment efficiency of baricitinib encapsulated PLGA nanoparticles.

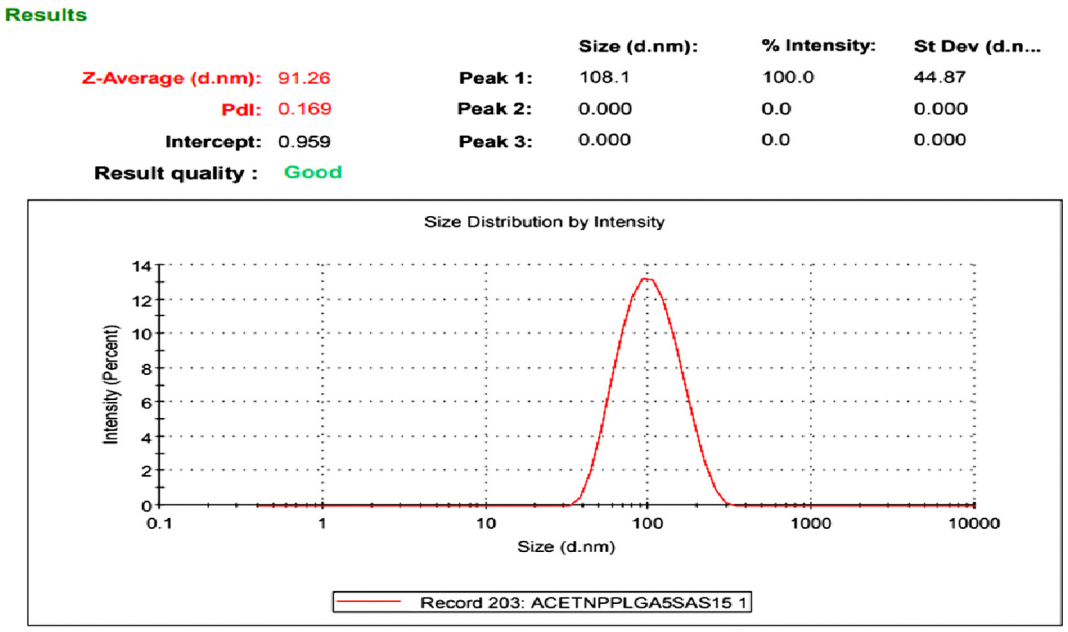

Fig. 6. Nanoparticle size analysis of formulation F8 obtained by Malvern zatasizer nano ZS.

the nanometer range while shape of the nanoparticles were found to be spherical. The sizes obtained in the SEM image are not consistent with those obtained in dynamic light scattering studies by zetasizer nano (Malvern, UK). The larger particles observed in the photomicrograph could be due to particle growth either during freeze drying or during sample preparation for imaging studies which involved dispersion of dried particles in the deionized water.

3.3.2. X-ray diffraction study of baricitinib encapsulated nanoparticles

The X-ray diffraction study of pure baricitinib and baricitinib encapsulated nanoparticles were performed to investigate particle nature of baricitinib before and after encapsulation. The XRD spectra of pure baricitinib and baricitinib encapsulated nanoparticles are presented in Fig. 9. The spectrum of pure baricitinib exhibited several characteristics sharp peaks between 12.5 and 42.5° with very high intensity from 200 counts reaching upto 1600 counts. These peaks are indicative of crystalline nature of the baricitinib (Fig. 9a). However, the spectrum of PLGA (Fig. 9b) did not exhibited peaks which is indicative of non-crystalline nature of the polymer. It has been reported that PLGA composed of L isomers of polylactic acid and polyglycolic acid are crystalline, whereas those composed of racemic mixtures i.e. both levo and dextro rotatory forms are amorphous in nature. Furthermore, PLGA copolymers composed of less than 70% glycolic acid are known to be amorphous (Dinarvand et al., 2011). In the present study, we used D, L-PLGA (50:50) which exhibited amorphous nature in our X-ray diffraction

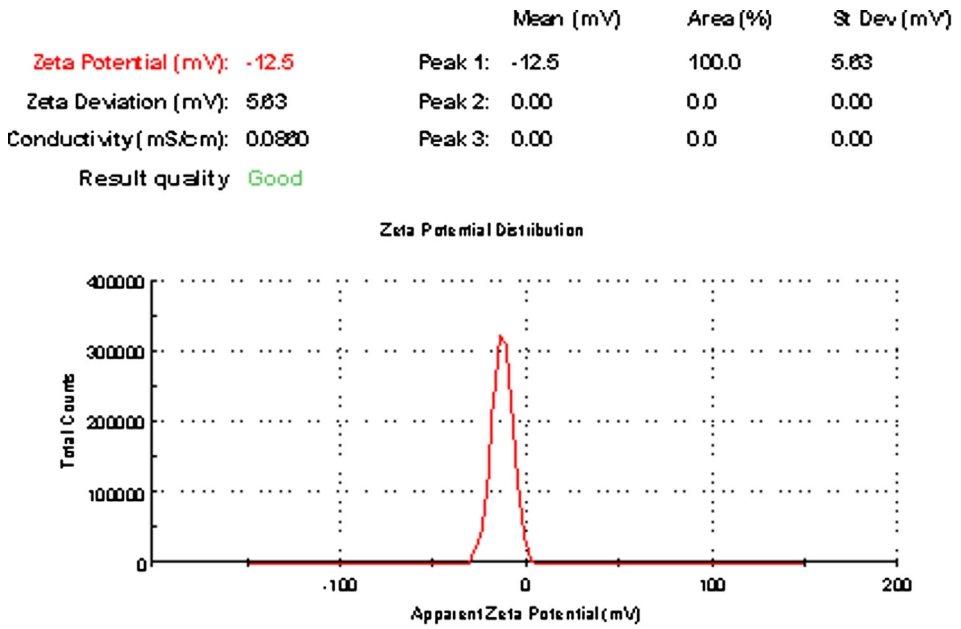

Fig. 7. Nanoparticle zeta-potential analysis of formulation F 8 obtained by Malvern zatasizer nano ZS.

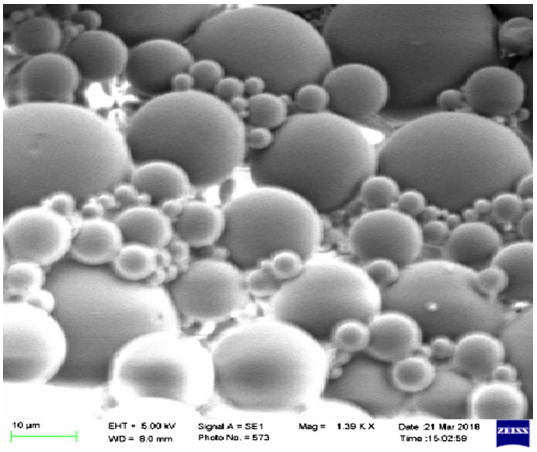

Fig. 8. Scanning Electron photomicrograph of baricitinib encapsulated PLGA nanoparticles (formulation F-8), Magnification:1390×, EHT: electron high tension; 5 kV, WD; working distance 8 mm.

study (Fig. 9b), showing consistency with the available literatures (You et al., 2005; Dinarvand et al., 2011). The XRD spectrum of baricitinib encapsulated PLGA nanoparticles (Fig. 9c) exhibited non-crystalline behaviour (amorphous nature) with almost no intense peak except 2 broad and diffused peaks with low intensity of approximately 385 and 393 counts at 19.3 and 23.2 degree respectively. This behaviour may be due to amorphization of crystalline baricitinib during nanoencapsulation within the PLGA polymer, causing loss of all high intensity peaks of crystalline baricitinib observed in Fig. 9a.

3.3.3. Differential Scanning calorimetry of nanoparticles

Differential Scanning calorimetry of pure baricitinib and baricitinib encapsulated nanoparticles was performed to compare the characteristics of baricitinib before and after nano-encapsulation. The DSC thermograms of baricitinib and baricitinib encapsulated nanoparticles are presented in Fig. 10. These DSC thermogram of baricitinib (Fig. 10b) exhibited sharp characteristic endotherm (melting point peak) at 215.3 °C. However, thermogram of baricitinib encapsulated nanoparticles (Fig. 10a) exhibited only a short endotherm at 55.3 °C, which correspond to the glass transition temperature (Tg) of the polymer PLGA. The absence of a sharp characteristic endothermic peak of baricitinib indicated the encapsulation of drug within the polymer. Furthermore, the drug may be molecularly dispersed as an amorphous mixture within the polymer. The melting point rage of the baricitinib reported in literature is between 212 and 215 °C (European Patent Application, 2018; Baricitinib: API STANDARDS, 2018). The melting point we observed in this study was 215.3 °C, which was very close to the reported values. Likewise, the glass transition temperature of polymer PLGA (50:50), we observed here (55.3 °C) is also very close to the reported values (45–55 °C) in the literature (Pyo Park and Jonnalagadda, 2006,).

3.3.4. Fourier transform infra-red spectroscopy of PLGA nanoparticles

FT-IR spectroscopy of pure baricitinib and PLGA nanoparticles encapsulated with baricitinib was performed to find out any chemical or molecular interaction between the baricitinib and PLGA polymer. The FT-IR spectra of baricitinib and baricitinib encapsulated PLGA nanoparticles are presented in Fig. 10. The FT-IR spectrum of baricitinib (Fig. 11a) exhibited several strong absorption bands at wavenumbers of 3203.18, 3117.37, 2847.38, 2256.31, 1857.43 and 1579.41 cm^{-1}, corresponding to N—H stretching, =C—H stretching (aromatic), —C—H stretching of the methyl/methylene groups, C≡N stretching, C=N stretching and C=C (aromatic) stretching respectively. The spectrum of baricitinib encapsulated nanoparticles (Fig. 11b), did not exhibited the characteristic absorption bands which were observed in the spectrum of baricitinib (Fig. 11a), rather two weak absorption bands at 2889.81 and 1760.69 cm^{-1}, which may be assigned to the —C—H stretching and C=O stretching of the methyl and carbonyl groups present in the PLGA polymer (Erbetta et al., 2012). The absence of characteristic absorption bands of baricitinib in the spectrum of PLGA nanoparticles indicates physical entrapment of baricitinib in the nanoparticles.

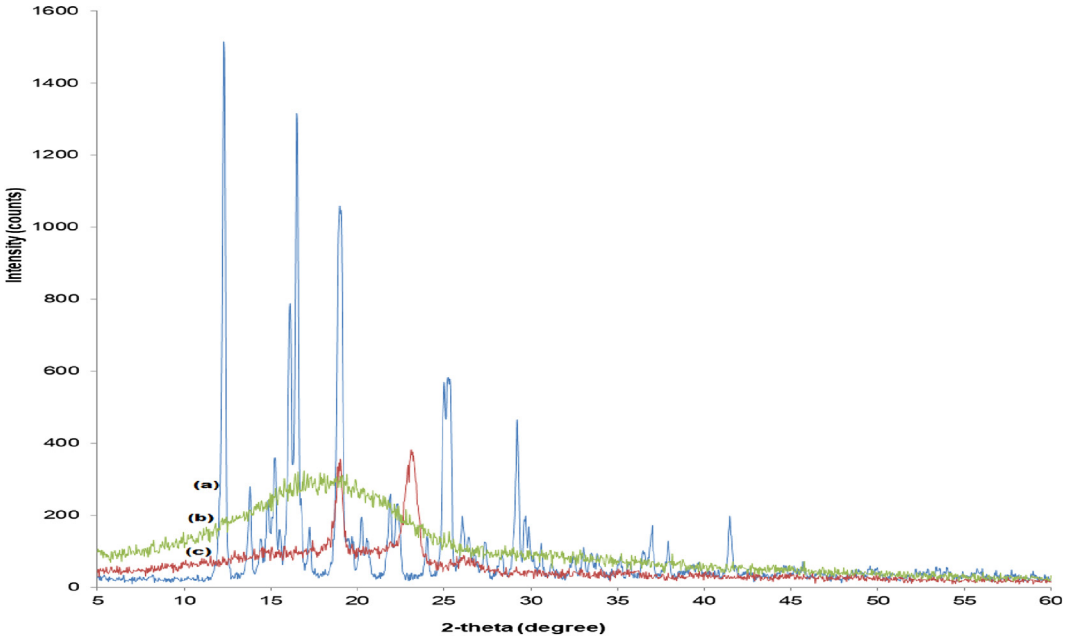

Fig. 9. X-ray diffractogram of (a) baricitinib, (b) PLGA and (c) baricitinib encapsulated PLGA nanoparticles.

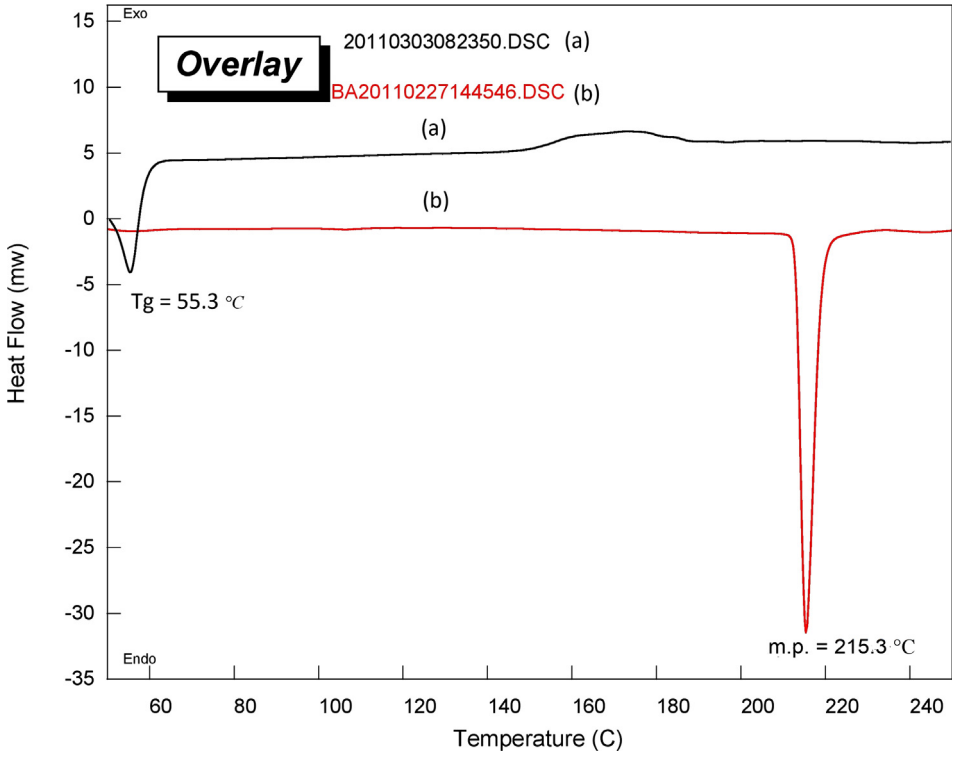

Fig 10. Differential Scanning calorimetry thermogram of (a) baricitinib encapsulated PLGA nanoparticles (b) baricitinib.

3.3.5. In vitro release study of baricitinib encapsulated PLGA nanoparticles

The *in vitro* release studies of baricitinib and baricitinib encapsulated PLGA nanoparticles were conducted in phosphate buffer pH 6.8 with 0.5% w/v of sodium lauryl sulphate to maintain the sink condition and to mimic the *in vivo* environment. The *in vitro* release profiles of pure baricitinib and baricitinib encapsulated PLGA nanoparticles (F-8) are shown in Fig. 12. The PLGA nanoparticles exhibited biphasic release pattern with an initial burst release of baricitinib (38%) within 2 h followed by slow release of drug over a period of 24 h (93%). The burst release of the baricitinib from nanoparticles may be due to adsorbed drug on the surface of the PLGA polymer. The drug release during the sustained release phase may result from slow degradation of PLGA in the dissolution media.

The *in vitro* release data were fitted to various kinetic models to understand the mechanism of release of baricitinib from the PLGA nanoparticles. The drug release profile for baricitinib encapsulated

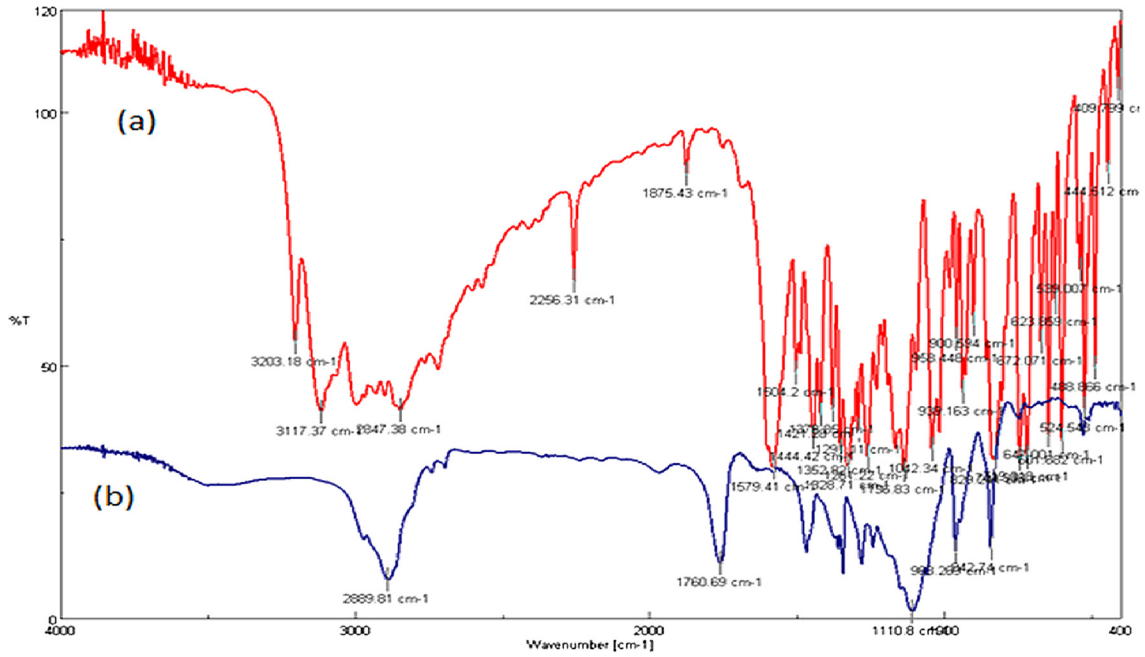

Fig 11. FT-IR Spectra of (a) baricitinib and (b) baricitinib encapsulated PLGA nanoparticles.

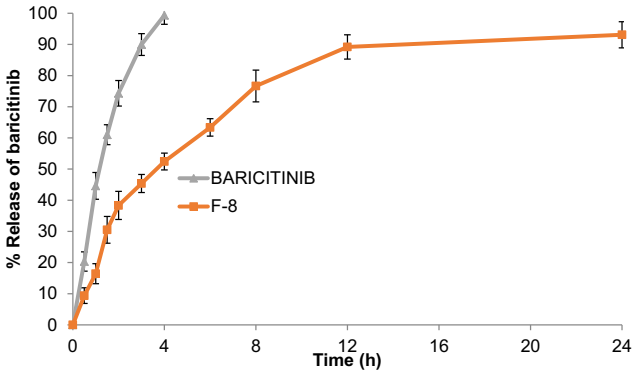

Fig. 12. *In vitro* release profiles of baricitinib (▲) and baricitinib encapsulated PLGA nanoparticles, formulation F-8 (■) in phosphate buffer pH 6.8 with 0.5% w/v sodium lauryl sulphate.

Table 5
Kinetic models with kinetic release rate constants and correlation coefficients of *in vitro* release profile of baricitinib encapsulated PLGA nanoparticles.

Kinetic models fitted	Correlation coefficients (R^2)	Release rate constants
Zero order	0.708	1.409
First order	0.911	0.279
Hixson-Crowell	0.854	0.627
Higuchi	0.918	0.549
Korsmeyer Peppas	0.563	0.026

nanoparticles was best fitted with Higuchi model as the regression coefficient (R2) was found to be the highest (0.918) for Higuchi model among the various kinetic models tested for the release profile (Table 5).

4. Conclusions

The baricitinib encapsulated PLGA nanoparticles produced by nanoprecipitation method had small size with very low PDI and good entrapment efficiency. *In vitro* release profile exhibited a sustained release behaviour resulting in 89% release in 12-h period while 93% over 24-h period. PLGA polymer had more pronounced effect on sustaining the drug release rather than enhancing the solubility of the drug encapsulated. This sustained release behavior may be utilized for the management of chronic rheumatoid arthritis and may be helpful in reduction of side effects by minimizing the dose of baricitinib. We plan to conduct an efficacy study and or bioavailability studies in the animals in near future.

Acknowledgments

The authors acknowledge the support given by Mr. Khalid Alhuwaisahl, under graduate pharmacy student, Dr. Mohammad Afroz Bakht and Imtiyaz Ali for X-ray Diffraction spectra and Dr. Faiyaz Shakeel for Scanning electron microscopy imaging.

Funding

This project has been funded by deanship of scientific research, Prince Sattam bin Abdulaziz University, Saudi Arabia, funding number-2017/03/7329.

Conflicts of interest

The authors declare no conflict of interest. The funders had no role in the design of the study; in the collection, analyses, or interpretation of data; in the writing of the manuscript, or in the decision to publish the results.

References

Aletaha, D., Neogi, T., Silman, A.J., Funovits, J., Felson, D.T., Bingham III, C.O., Birnbaum, N.S., Burmester, G.R., Bykerk, V.P., Cohen, M.D., Combe, B., 2010. 2010 rheumatoid arthritis classification criteria: an American College of Rheumatology/European League Against Rheumatism collaborative initiative. Arthritis Rheumatol. 62 (9), 2569–2581. https://doi.org/10.1002/art.27584.

Alshehri, S., Shakeel, F., Ibrahim, M., Elzayat, E., Altamimi, M., Shazly, G., Mohsin, K., Alkholief, M., Alsulays, B., Alshetaili, A., Alshahrani, A., Almalki, B., Alanazi, F., 2017. Influence of the microwave technology on solid dispersions of mefenamic acid and flufenamic acid. PLoS One 12 (7), e0182011. https://doi.org/10.1371/journal.pone.0182011.

Ansari, M.J., 2016. Preparation and evaluation of di-component and tri-component molecular inclusion complexes of silymarin. Lat. Am. J. Pharm. 35, 604–608 http://latamjpharm.org/previous_issue.php?vol=35&num=3.

Ansari, M.J., 2017. Factors affecting preparation and properties of nanoparticles by nanoprecipitation method. Indo Am. J. Pharm. Sci. 4 (12), 4854–4858. https://doi.org/10.5281/zenodo.1134425.

Assessment report: Olumiant. Available online: <https://www.ema.europa.eu/documents/assessment-report/olumiant-epar-public-assessment-report_en.pdf> (accessed on 10–24–2018).

Baricitinib: API standards. Available online: <https://www.clearsynth.com/en/CST48553.html> (accessed on 10–27–2018).

Baricitinib: technical information. Available online: <https://www.scbt.com/scbt/product/baricitinib-1187594-09-7> (accessed on 10–24–2018).

Costabile, G., Gasteyer, K.I., Nadithe, V Van, Denburgh, K., Lin, Q., Sharma, S., Reineke, J.J., Firestine, S.M., Merkel, O.M., 2018. Physicochemical and in vitro evaluation of drug delivery of an antibacterial synthetic benzophenone in biodegradable PLGA nanoparticles. AAPS PharmSciTech. https://doi.org/10.1208/s12249-018-1187-9. Sep 25.

Dahan, A., Miller, J.M., 2012. The solubility–permeability interplay and its implications in formulation design and development for poorly soluble drugs. AAPS J 14 (2), 244–251. https://doi.org/10.1208/s12248-012-9337-6.

Dinarvand, R., Sepehri, N., Manoochehri, S., Rouhani, H., Atyabi, F., 2011. Polylactide-co-glycolide nanoparticles for controlled delivery of anticancer agents. Int. J. Nanomed. 6, 877–895. https://doi.org/10.2147/IJN.S18905.

Drug Approval Package: Olumiant baricitinib. Available online: <https://www.accessdata.fda.gov/drugsatfda_docs/nda/2018/207924Orig1s000TOC.cfm> (accessed on 10–24–2018).

Drugbank: identification of baricitinib, 2018. Available online: <https://www.drugbank.ca/drugs/DB11817> (accessed on 10–24–2018).

Erbetta, C.D.A.C., Alves, R.J., Resende, J.M., de Souza Freitas, R.F., de Sousa, R.G., 2012. Synthesis and characterization of poly (D, L-lactide-co-glycolide) copolymer. J. Biomater. Nanobiotechnol. 3 (02), 208–225. https://doi.org/10.4236/jbnb.2012.32027.

European Patent Application. Available online: <https://data.epo.org/publication-server/rest/v1.0/publication-dates/20180117/patents/EP3269719NWA1/document.pdf> (accessed on 10–27–2018).

Fessi, H., Puisieux, F., Devissaguet, J.P., Ammoury, N., Benita, S., 1989. Nanocapsule formation by interfacial polymer deposition following solvent displacement. Int. J. Pharm. 55 (1), R1–R4. https://doi.org/10.1016/0378-5173(89)90281-0.

Finsy, R., De Jaeger, N., 1991. Particle sizing by photon correlation spectroscopy. Part II: Average values. Part. Part. Syst. Charact. 8 (1–4), 187–193. https://doi.org/10.1002/ppsc.19910080135.

Honary, S., Zahir, F., 2013. Effect of zeta potential on the properties of nano-drug delivery systems-a review (Part 2). Trop. J. Pharm. Res. 12 (2), 265–273. https://doi.org/10.4314/tjpr.v12i2.19.

Huang, W., Zhang, C., 2018. Tuning the size of poly (lactic-co-glycolic acid) (PLGA) nanoparticles fabricated by nanoprecipitation. Biotechnol. J. 13 (1), 1700203–1700211. https://doi.org/10.1002/biot.201700203.

Jiang, J., Oberdörster, G., Biswas, P., 2009. Characterization of size, surface charge, and agglomeration state of nanoparticle dispersions for toxicological studies. J. Nanopart. Res. 11 (1), 77–89. https://doi.org/10.1007/s11051-008-9446-4.

Joshi, G., Kumar, A., Sawant, K., 2016. Bioavailability enhancement, Caco-2 cells uptake and intestinal transport of orally administered lopinavir-loaded PLGA nanoparticles. Drug Del. 23 (9), 3492–3504. https://doi.org/10.1080/10717544.2016.1199605.

Makadia, H.K., Siegel, S.J., 2011. Poly lactic-co-glycolic acid (PLGA) as biodegradable controlled drug delivery carrier. Polymers 3 (3), 1377–1397. https://doi.org/10.3390/polym3031377.

Mu, L., Feng, S.S., 2003. A novel controlled release formulation for the anticancer drug paclitaxel (Taxol®): PLGA nanoparticles containing vitamin E TPGS. J. Controlled Release 86 (1), 33–48. https://doi.org/10.1016/S0168-3659(02)00320-6.

Product information: baricitinib. Available online <https://www.caymanchem.com/pdfs/16707.pdf> (accessed on 10–24–2018).

Pyo Park, P.I., Jonnalagadda, S., 2006. Predictors of glass transition in the biodegradable poly-lactide and poly-lactide-co-glycolide polymers. J. Appl. Polym. Sci. 100 (3), 1983–1987. https://doi.org/10.1002/app.22135.

Rafiei, P., Haddadi, A., 2017. Pharmacokinetic consequences of PLGA nanoparticles in docetaxel drug delivery. Pharm. Nanotechnol. 5 (1), 3–23. https://doi.org/10.2174/2211738505666161230110108.

Sahu, B.P., Das, M.K., 2014. Nanosuspension for enhancement of oral bioavailability of felodipine. App. Nanosci. 4 (2), 189–197. https://doi.org/10.1007/s13204-012-0188-3.

Shen, J., Burgess, D.J., 2013. In vitro dissolution testing strategies for nanoparticulate drug delivery systems: recent developments and challenges. Drug Del. Transl. Res 3 (5), 409–415. https://doi.org/10.1007/s13346-013-0129-z.

Singh, G., Pai, R.S., 2014. Optimized PLGA nanoparticle platform for orally dosed trans-resveratrol with enhanced bioavailability potential. Expert Opin. Drug Deliv. 11 (5), 647–659. https://doi.org/10.1517/17425247.2014.890588.

Venkatesh, D.N., Baskaran, M., Karri, V.V.S.R., Mannemala, S.S., Radhakrishna, K., Goti, S., 2015. Fabrication and in vivo evaluation of Nelfinavir loaded PLGA nanoparticles for enhancing oral bioavailability and therapeutic effect. Saudi Pharm. J. 23 (6), 667–674. https://doi.org/10.1016/j.jsps.2015.02.021.

Win, K.Y., Feng, S.S., 2005. Effects of particle size and surface coating on cellular uptake of polymeric nanoparticles for oral delivery of anticancer drugs. Biomaterials 26 (15), 2713–2722. https://doi.org/10.1016/j.biomaterials.2004.07.050.

You, Y., Min, B.M., Lee, S.J., Lee, T.S., Park, W.H., 2005. In vitro degradation behavior of electrospun polyglycolide, polylactide, and poly (lactide-co-glycolide). J. Appl. Polym. Sci. 95 (2), 193–200. https://doi.org/10.1002/app.21116.